Importance of F_1-ATPase Residue α-Arg-376 for Catalytic Transition State Stabilization†

Sashi Nadanaciva, Joachim Weber, Susan Wilke-Mounts, and Alan E. Senior*

Department of Biochemistry and Biophysics, Box 712, University of Rochester Medical Center, Rochester, New York 14642

Received July 29, 1999; Revised Manuscript Received September 20, 1999

ABSTRACT: The functional role of essential residue α-Arg-376 in the catalytic site of F_1-ATPase was studied. The mutants αR376C, αR376Q, and αR376K were constructed, and combined with the mutation βY331W, to investigate catalytic site nucleotide-binding parameters, and to assess catalytic transition state formation by measurement of MgADP−fluoroaluminate binding. Each mutation caused large impairment of ATP synthesis and hydrolysis. Despite the apparent proximity of α-Arg-376 to bound nucleoside di- and triphosphate in published X-ray structures, the mutations had little effect on MgADP or MgATP binding affinities, particularly at the highest affinity catalytic site, site 1. Both Cys and Gln mutants abolished transition state formation, demonstrating that α-Arg-376 is normally involved at this step of catalysis. A model of the F_1-ATPase catalytic transition state structure is presented and discussed. The Lys mutant, although severely impaired, supported transition state formation, suggesting that an additional essential role for the α-Arg-376 guanidinium group exists, likely in α/β conformational signal transmission required for steady-state catalysis. Parallels between α-Arg-376 and GAP/G-protein "arginine finger" residues are evident.

The ATP synthase (F_1F_o-ATPase) of bacterial, mitochondrial, and thylakoid membranes synthesizes ATP from ADP and P_i during oxidative and photophosphorylation using a proton-motive force as energy source. In bacteria, it also hydrolyzes ATP to generate a proton gradient for nutrient uptake and flagellar rotation (*1*, *2*). The catalytic F_1 sector of ATP synthase has the subunit composition $\alpha_3\beta_3\gamma\delta\epsilon$ and contains three catalytic nucleotide-binding sites which alternate with three noncatalytic nucleotide-binding sites in the hexagonal $\alpha_3\beta_3$ structure (*3*). F_1 is connected to the membrane-spanning, proton-conducting sector, F_o, by "stalk" subunits. Isolated F_1 retains ATPase activity in the absence of F_o, and has been used extensively as a model for studying the catalytic mechanism. Addition of a substoichiometric amount of substrate MgATP to F_1 results in tight binding at only one catalytic site, followed by a single turnover of hydrolysis and slow product release (*4*). Catalysis is accelerated 10^5-fold to reach physiological rates when sufficient MgATP is added to fill all three catalytic sites (*2*, *5*, *6*). Under these steady-state conditions, rotation of the central γ subunit relative to the $\alpha_3\beta_3$ complex occurs (*7*), which is thought to be correlated with concerted changes in the binding affinity of the catalytic sites for substrates and products (*8*).

Recent X-ray structures of bovine mitochondrial F_1 (*3*), rat liver mitochondrial F_1 (*9*), and the $\alpha_3\beta_3$ complex from the thermophilic bacterium PS3 (*10*) have provided detailed views of the nucleotide-binding sites of ATP synthase at the molecular level. The three catalytic sites lie at α/β interfaces, with most of the nucleotide-binding residues being contributed by β subunits. Interestingly, however, the structures revealed that one of the residues potentially involved in interacting with nucleotide at the catalytic sites is an arginine residue provided by the α subunit, namely, α-Arg-376.[1] The crystal structure of bovine mitochondrial F_1 (*3*) shows that α-Arg-376 (α-Arg-373 in bovine) lies straddled across the catalytic α/β interface with its side chain located close to the phosphate groups of catalytic site-bound nucleotide. Abrahams et al. (*3*) speculated that the guanidinium group of α-Arg-376 could help stabilize the negative charges that develop at the terminal phosphate of a pentacoordinate catalytic transition state species. In view of crystallographic studies of G-proteins and their GAPs (GTPase activating proteins), which have highlighted the importance of inserted "arginine finger" residues in stabilizing the transition state and thereby greatly accelerating the catalytic reaction in the G-proteins (*11*−*13*), it is tantalizing to consider that α-Arg-376 may have a comparable role in ATP synthase.

Prior to the information revealed by the X-ray structures of F_1, Soga et al. (*14*) and Turina et al. (*15*) had shown that the mutation αR376C abolishes both ATP synthesis and ATPase activity, indicating that α-Arg-376 is essential for catalysis. However, somewhat at variance with the X-ray structural data, these workers suggested that α-Arg-376 may be one of several residues at the α/β interface necessary for transmitting conformational changes during cooperative, steady-state catalysis, rather than being crucial for ATP hydrolysis per se.

To acquire a clearer understanding of the role of α-Arg-376 in F_1-ATPase, we constructed three mutations, αR376Q, αR376C, and αR376K, and combined each with the mutation βY331W. The aromatic ring of the β-331 residue forms van

† Supported by NIH Grant GM25349 to A.E.S.

* Correspondence should be addressed to this author. Phone: 716-275-2777. Fax: 716-271-2683. E-mail: alan_senior@urmc.rochester.edu.

[1] *E. coli* residue numbering is used throughout.

10.1021/bi9917683 CCC: $18.00
Published on Web 11/05/1999

der Waals interactions with the adenine ring of bound nucleotide at the catalytic site, and acts as an intrinsic fluorescent probe sensitive to nucleotide binding (*1*). The strong fluorescence signal of β-Trp-331 is quenched completely upon addition of saturating amounts of nucleotide, enabling catalytic site nucleotide-binding parameters to be determined. In this paper, we examined MgATP, ATP, and MgADP binding properties of αR376C/βY331W, αR376Q/βY331W, and αR376K/βY331W F_1, and investigated whether these mutant enzymes could bind the transition state analogue MgADP−fluoroaluminate. Based on the results obtained here and on recent data from our laboratory (*16, 17*), we propose a model for the catalytic transition state of F_1-ATPase and its formation.

EXPERIMENTAL PROCEDURES

Construction of Mutant E. coli Strain αR376C/βY331W. A 1.2 kb *Xho*I−*Csp*45I fragment containing the αR376C mutation was moved from plasmid pRL3 (*15*) into plasmid pSWM4 (*5*), which contains the mutation βY331W, to generate plasmid pSWM71 (αR376C/βY331W). pSWM71 was introduced into strain AN888 (*18*) to generate strain SWM71.

Construction of Mutant E. coli Strains αR376Q/βY331W and αR376K/βY331W. Site-directed mutagenesis was done according to the method of Vandeyar et al. (*19*). Template DNA was M13mp18 containing a 1.4 kb *Sph*I−*Sal*I fragment from plasmid pSWM4. The mutagenic oligonucleotide for the αR376Q mutation was TT TCC GTA TCC **CAG** GTT GGT GGT where the boldface letters represent the mutation Arg→Gln (CGT→CAG) and introduce a *Bst*XI restriction site used for identifying the mutation. DNA sequencing confirmed the presence of the αR376Q mutation and ruled out the presence of any undesired mutation. The mutagenic ologonucleotide for the αR376K mutation was TT TCC GTA TCC **AAA** GTT GGT GGT where the boldface letters represent the mutation Arg→Lys (CGT→AAA). DNA sequencing identified the αR376K mutation and ruled out the presence of any undesired mutation. A 1 kb *Sfi*I−*Bst*BI fragment containing the αR376Q or αR376K mutation was moved from replicative form phage to pSWM4 to generate new plasmids pSWM77 (αR376Q/βY331W) and pSWM74 (αR376K/βY331W). pSWM77 and pSWM74 were introduced into strain AN888 to generate strain SWM77 and strain SWM74. However, the yield of F_1 isolated from both these strains was very low (<0.02 mg/g wet weight of cells). Since the plasmid pBWU13.4 and its derivatives are known to produce high yields of F_1 when expressed in the *E. coli* strain DK8 (*17, 20*), a 3.3 kb *Xho*I−*Eag*I fragment from pBWU13.4 was replaced by the corresponding fragment from pSWM77 and pSWM74 to generate plasmids pSN3 (αR376Q/βY331W) and pSN4 (αR376K/βY331W), respectively. pSN3 and pSN4 were each introduced into DK8 to generate strains SN3 and SN4, respectively. Both these strains produced superior yields of F_1 (0.25 mg/g wet weight of cells).

Characterization of Mutant E. coli Strains. Growth analyses of *E. coli* strains both in limiting (3 mM) glucose liquid medium and on solid succinate plates were performed as described earlier (*21*).

Enzyme Purification and Characterization. αR376C/βY331W F_1 from strain SWM71, αR376Q/βY331W F_1 from strain SN3, αR376K/βY331W F_1 from strain SN4, βY331W F_1 from strain SWM4 (*5*), and wild-type F_1 from strain SWM1 (*22*) were purified as described in ref *23*. Purity and subunit composition of enzymes were determined by SDS-gel electrophoresis (*24*). Protein concentration was determined by the method of Bradford (*25*). Specific ATPase activity measurements were carried out in 50 mM Tris−SO_4, pH 8.5, 4 mM $MgCl_2$, 10 mM NaATP. Phosphate release was determined as described in ref *26*.

Fluorescence Measurements. An Aminco-Bowman 2 spectrofluorometer or a SPEX Fluorolog 2 fluorometer was used to measure tryptophan fluorescence. Excitation and emission wavelengths were 295 and 360 nm, respectively, and all measurements were done at 23 °C. For determination of the tryptophan content of the mutant enzymes, 100−200 nM mutant F_1 and wild-type F_1 were each incubated in 6.3 M guanidine hydrochloride for 45 min, and the fluorescence emission was compared at 360 nm. For determination of nucleotide-binding parameters by titration, βY331W F_1 was first depleted of catalytic site nucleotide by sequential passage through two 1 mL Sephadex G-50 columns in 50 mM Tris−SO_4, pH 8.0, at 23 °C (*27*). For the three αR376 mutant enzymes, all titrations were done using nucleotide-depleted enzyme (depleted of endogenous nucleotide from noncatalytic as well as catalytic sites) which was prepared as described in ref *28*. The final enzyme concentration for each titration was 40−100 nM. MgATP and MgADP titrations were done in 50 mM Tris−SO_4, pH 8.0, 2.5 mM $MgSO_4$, with NaATP or NaADP added as indicated. ATP and ADP titrations were done in 50 mM Tris−SO_4, pH 8.0, 0.5 mM EDTA, with NaATP or NaADP added at increasing concentrations. MgADP titrations in the presence of fluoroaluminate were done in 50 mM Tris−SO_4, pH 8.0, 2.5 mM $MgSO_4$, 0.5 mM $AlCl_3$, 10 mM NaF, with NaADP added at increasing concentrations. Inner filter and volume effects were corrected by doing parallel titrations with wild-type F_1, and background signals due to buffer were subtracted. Nucleotide-binding parameters were determined from computer-generated fits to the measured data using equations described in ref *29*.

RESULTS

Functional Effects of αR376C/βY331W, αR376Q/βY331W, and αR376K/βY331W Mutations. Growth yields of the three mutant strains were tested in liquid medium containing limiting glucose. All three strains had growth yields similar to that of the negative (Unc^-) control, demonstrating that ATP synthesis was severely reduced by mutating α-Arg-376. (The βY331W mutation itself had no significant effect on growth yield.) None of the mutants grew on solid succinate medium, confirming that the αR376 mutations abolished oxidative phosphorylation. ATPase activity in membranes prepared from each strain was very low and not significantly different from that of Unc^- control membranes.

Properties of Purified F_1 from αR376C/βY331W, αR376Q/βY331W, and αR376K/βY331W Mutants. Purified F_1 isolated from the three mutant strains had a molecular size similar to wild-type F_1 as judged from the Sephacryl S300 elution profile obtained during the final purification step. SDS−polyacrylamide gel electrophoresis of the mutant enzymes showed that they had subunit compositions identical to wild-

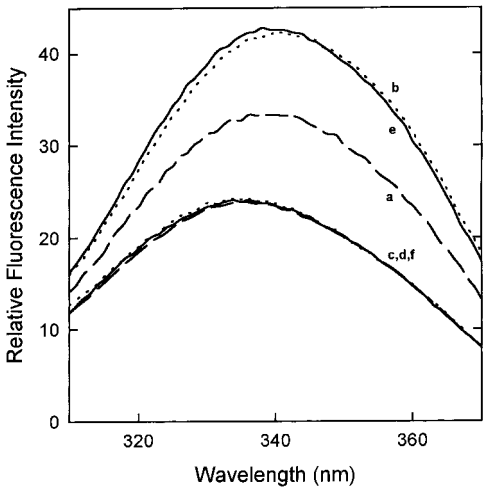

FIGURE 1: Tryptophan fluorescence spectra of mutant enzymes. Equal concentrations of purified mutant F_1 (84 nM) in 50 mM Tris−SO_4, pH 8.0, were compared. Excitation was at 295 nm. For details of how the enzymes were prepared, see text. Curve a, αR376K/βY331W, prepared by passage through two centrifuge columns; curve b, βY331W, prepared by passage through two centrifuge columns; curves c and d, after addition of 2.5 mM MgATP to curves a and b, respectively; curve e, αR376K/βY331W, nucleotide-depleted; curve f, after addition of 2.5 mM MgATP to curve e. The data for the αR376C/βY331W and αR376Q/βY331W enzymes are not shown, but were very similar to those for αR376K/βY331W.

type F_1. Purity was confirmed by analysis of the tryptophan content of the three mutant enzymes. The values found ranged from 12.0 to 12.7 mol of Trp/mol of F_1, consistent with the expected value of 12. Specific ATPase activities of purified enzymes were as follows: wild-type, 28 units/mg; αR376C/βY331W, 0.006 unit/mg; αR376Q/βY331W, 0.009 unit/mg; αR376K/βY331W, 0.027 unit/mg. [It has been established previously (*5*) that βY331W F_1 has a specific ATPase activity equal to 50% of wild-type F_1.] Thus, the three αR376 mutant enzymes had specific ATPase activities that were <0.1% of wild-type F_1. The data for the αR376C/βY331W are in agreement with data on the αR376C mutant alone (*14*, *15*); data for αR376Q and -K mutants have not been reported previously. Clearly, α-Arg-376 is crucial for catalysis, and even the conservative Lys substitution impaired steady-state catalysis severely.

Tryptophan Fluorescence Spectra of αR376C/βY331W F_1, αR376Q/βY331W F_1, and αR376K/βY331W F_1. In past work we found that sequential passage of βY331W F_1 through two 1 mL Sephadex G-50 centrifuge columns in 50 mM Tris−SO_4, pH 8.0, at 23 °C, was sufficient to remove all catalytic site bound nucleotide (*16*, *27*). Here, however, with the three αR376 mutant enzymes, this was found not to be the case. The enzymes were passed through two centrifuge columns as described; then the fluorescence spectrum of each was compared with that of similarly treated βY331W enzyme. All three mutant enzymes behaved the same way, and Figure 1 shows the results for αR376K/βY331W F_1. It is seen that the fluorescence emission at 360 nm of the αR376K/βY331W enzyme (curve a) was lower in comparison to βY331W (curve b). Upon addition of saturating (2.5 mM) MgATP, the fluorescence signals of both enzymes were quenched to a similar level (curves c and d), which corresponds to that of wild-type F_1. These results indicated that each of the three mutant enzymes, αR376C/βY331W, αR376Q/βY331W, and αR376K/βY331W, retained nucleotide at approximately one catalytic site after passage through two centrifuge columns. Why this is the case is not yet clear. As noted below, nucleotide-binding affinities of the mutants were not uniformly higher than wild-type. However, to overcome the problem, we prepared "nucleotide-depleted" enzymes [involving passage through a 100 × 0.9 cm column of Sephadex G-50 in 50% (v/v) glycerol-containing buffer as described in ref *28*] to remove all catalytic and noncatalytic site bound nucleotide. After nucleotide-depletion, all three enzymes again behaved the same. As seen in Figure 1, curve e, the Trp fluorescence spectrum of nucleotide-depleted αR376K/βY331W enzyme was now similar to that of βY331W F_1 (curve b), and 2.5 mM MgATP quenched the fluorescence signal to the same level as before (curve f), demonstrating that all three catalytic sites were empty in the nucleotide-depleted enzyme, and could be filled by 2.5 mM MgATP. In the rest of this work, nucleotide-depleted αR376 mutant enzymes were used. We confirmed that the nucleotide-depletion procedure did not significantly change the specific ATPase activity of any of the mutant enzymes.

Nucleotide-Binding Properties of αR376Q/βY331W F_1. Figure 2A shows binding of MgATP to αR376Q/βY331W and βY331W F_1. The data were found to fit well to a model using three different binding sites (lines in Figure 2A), consistent with what we have found previously for MgATP binding (*5*, *29*). The calculated dissociation constants are given in Table 1. It is clear from Figure 2A that there is no significant difference between the titration curves, demonstrating that the mutation αR376Q did not significantly affect MgATP binding at any of the three catalytic sites.

Figure 2B shows titration curves for ATP binding (absence of Mg^{2+}) to αR376Q/βY331W and βY331W. Here the solid lines are computer-generated fits using a model for a single class of binding site, which we have found to be appropriate for ATP binding to βY331W in previous work (*5*, *29*). The calculated K_d value (Table 1) for αR376Q/βY331W F_1 was 103 μM (the corresponding K_d for βY331W F_1 is 71 μM), and the calculated total number of binding sites, *N*, was 2.6 (2.9 for βY331W F_1). The dotted line in Figure 2B is a fit to a model using three different binding sites, which for the αR376Q/βY331W mutant enzyme was more satisfactory, and gave values as follows: $K_{d1} = 14$ μM, $K_{d2,3} = 335$ μM. Overall, the data show that ATP binding was not significantly impaired by the αR376Q mutation.

MgADP titration curves for αR376Q/βY331W and βY331W F_1 are shown in Figure 2C. It is evident that the two curves are similar, indicating that the αR376Q mutation did not alter MgADP binding significantly. The lines are computer-generated fits to a model using two classes of binding sites, which we have found to be satisfactory for MgADP binding in previous work (*5*, *29*). Calculated K_d values are given in Table 1. The *N* values for the two classes of sites occupied by MgADP were N_1 (high affinity) = 1.1 and N_2 (lower affinity) = 1.6 for αR376Q/βY331W F_1; the corresponding values for βY331W F_1 were 0.9 and 1.8.

Summarizing, the αR376Q mutation did not significantly affect MgATP, ATP, or MgADP binding at any of the catalytic sites, demonstrating that the guanidinium group of α-Arg-376 is not obligatory for binding any of these nucleotides.

Nucleotide-Binding Properties of αR376C/βY331W F_1. Nucleotide-binding parameters were determined from titra-

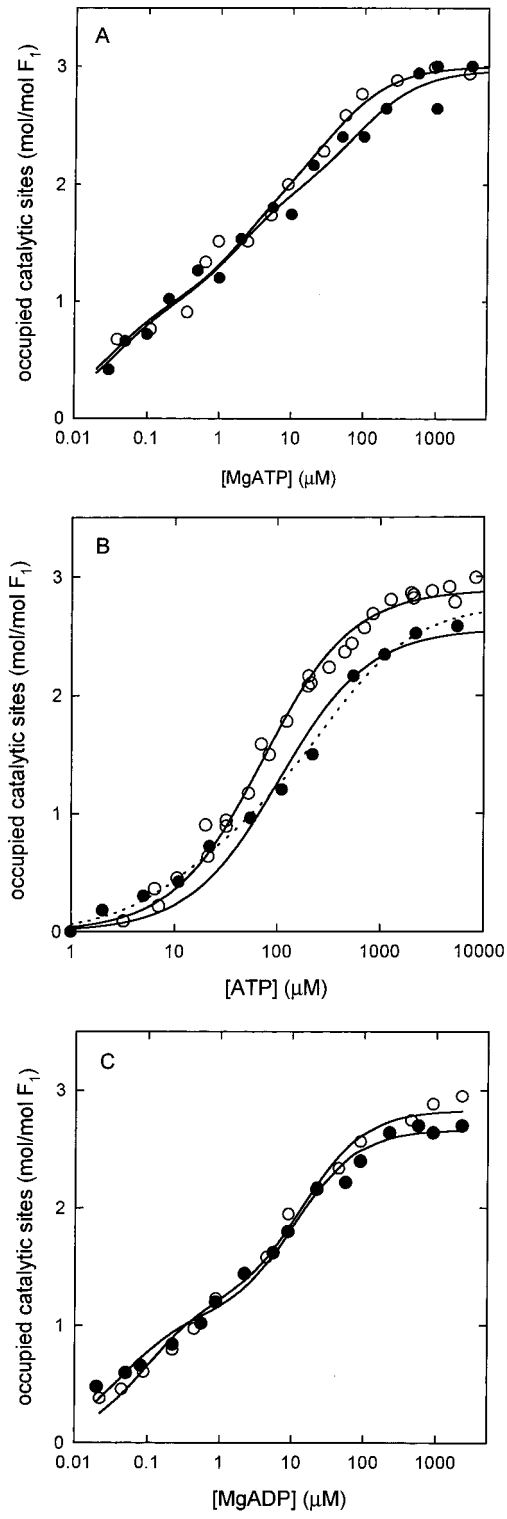

FIGURE 2: Binding of nucleotide to αR376Q/βY331W F_1. (A) MgATP titration; (B) ATP titration (absence of Mg^{2+}); (C) MgADP titration. (○) βY331W F_1; (●) αR376Q/βY331W F_1. The lines are computer-generated fits to a model assuming three different sites (A), a single class of sites (closed circles, solid line) or three different sites (closed circles, dotted line) (B), and two classes of sites (C).

tion curves as in Figure 2, and the results obtained are given in Table 1. For MgATP binding to αR376C/βY331W F_1, a model with three different binding sites gave a good fit to the data, and the calculated K_d values (Table 1) indicated that the αR376C mutation had little effect on MgATP binding affinity at catalytic site 1 (the highest affinity site, where catalysis is expected to occur) but reduced the binding affinity by 10-fold and 7-fold at sites 2 and 3, respectively. For ATP binding, a model with a single class of binding sites fitted the data well. ATP binding affinity was greatly reduced by the αR376C mutation, and even at 10 mM, ATP saturation was not achieved. The calculated K_d was 14-fold higher (Table 1) than the corresponding K_d for ATP binding to βY331W F_1. The MgADP titration curve indicated that the αR376C mutation caused slight impairment of MgADP binding (Table 1).

Table 1: Catalytic Site Nucleotide-Binding Parameters of αR376Q/βY331W, αR376C/βY331W, and αR376K/βY331W F_1[a]

	αR376Q/βY331W	αR376C/βY331W	αR376K/βY331W	βY331W
MgATP				
K_{d1}	0.03	0.05	0.03	0.028[b]
K_{d2}	2.0	21.7	0.21	2.1
K_{d3}	88	256	32	39
ATP				
K_{d1},K_{d2},K_{d3}	103[c]	972	27[d]	71[e]
MgADP				
K_{d1}	0.04	0.29	0.05	0.08[f]
K_{d2},K_{d3}	11.1	30.6	7.2	14.0

[a] K_d values in micromolar. [b] From ref *30*. [c] Calculated for a single class of sites (Figure 2B). A model using three different sites gave K_{d1} = 14 μM; K_{d2}, K_{d3} = 335 μM (see Results). [d] Calculated for a single class of sites. A model using three different sites gave K_{d1} = 4 μM; K_{d2}, K_{d3} = 70 μM (see Results). [e] From ref *5*. [f] From ref *16*.

The decreased affinity for MgATP at sites 2 and 3 may be due to repulsion of the γ-phosphate of MgATP at these sites if the Cys side chain is partly negatively charged at the pH at which the binding measurements were done (pH 8.0). The more pronounced decrease in affinity for ATP is consistent with this idea, since greater repulsion caused by the two additional negative charges of ATP would be expected.

Nucleotide-Binding Properties of αR376K/βY331W F_1. Nucleotide-binding parameters were determined from titration curves as in Figure 2, and the results obtained are given in Table 1. For MgATP binding to αR376K/βY331W F_1, a model using three different binding sites fitted the data well. As Table 1 shows, the αR376K mutation did not impair MgATP binding at any of the catalytic sites (K_{d1} and K_{d3} were similar to the corresponding K_d values for βY331W F_1) and, in fact, caused tighter binding at site 2 (K_{d2} was decreased by 10-fold in comparison with βY331W F_1). For ATP binding, a model using a single class of binding sites gave a calculated K_d of 27 μM for αR376K/βY331W F_1, indicating that the ATP binding affinity was somewhat increased by the αR376K mutation. However, a model using three different binding sites fitted the data better and gave values of K_{d1} = 4 μM, K_{d2} = 70 μM, and K_{d3} = 70 μM. Thus, using the second model, the αR376K mutation caused tighter binding of ATP at site 1 (by 17-fold) while the ATP-binding affinity at sites 2 and 3 was similar to βY331W F_1. For MgADP binding, a model using two classes of binding sites fitted the data well. Calculated dissociation constants are given in Table 1.

Summarizing, the αR376K mutation did not impair MgATP, ATP, or MgADP binding at any of the catalytic sites, and actually increased binding affinity somewhat in certain instances.

MgADP−Fluoroaluminate Binding to αR376Q/βY331W, αR376C/βY331W, and αR376K/βY331W F_1. Measurement of binding of the catalytic transition state analogue MgADP−fluoroaluminate by the fluorescence technique was recently shown to be a convenient and sensitive method that allows detection of formation of the catalytic transition state in wild-type and mutant F_1 (*16, 17*). In βY331W F_1, fluoroaluminate greatly enhances MgADP binding affinity at catalytic site 1 (K_{d1} decreased from 0.08 μM to ≪1 nM), has a lesser effect at site 2, and has no effect at site 3, leading to the conclusions that MgADP−fluoroaluminate forms a catalytic transition state-like structure at site 1, and perhaps a partial transition state-like structure at site 2, but does not bind at site 3 (*16*). In contrast, enzymes with mutations at residues β-Lys-155, β-Arg-182, and β-Glu-181, all of which had negligible ATPase activity, were unable to form the catalytic transition state (*16, 17*). As noted in the introduction, Abrahams et al. (*3*) have suggested that α-Arg-376 could be involved in stabilizing the transition state in F_1. We therefore investigated binding of MgADP−fluoroaluminate to the αR376 mutant enzymes.

Figure 3A shows titration curves for MgADP binding to αR376Q/βY331W F_1 in the presence and absence of $AlCl_3$ and NaF. It is obvious that both curves are similar, showing that fluoroaluminate did not alter MgADP binding affinity at any of the catalytic sites. Hence, the αR376Q mutation prevented formation of the catalytic transition state. The same result was obtained with αR376C/βY331W F_1 (data not shown), demonstrating that this enzyme, like αR376Q/βY331W, could not form the transition state.

In contrast, the αR376K/βY331W F_1 did show substantial enhancement of MgADP binding by fluoroaluminate (Figure 3B), similar to what is seen with βY331W (*16*). Thus, the conservative Lys substitution apparently had the capability to support formation of the catalytic transition state. It may be noted that since the binding of MgADP−fluoroaluminate at site 1 is so very tight we cannot calculate actual K_d values; hence, we cannot say whether the Lys substitution is actually equal to Arg in supporting this function.

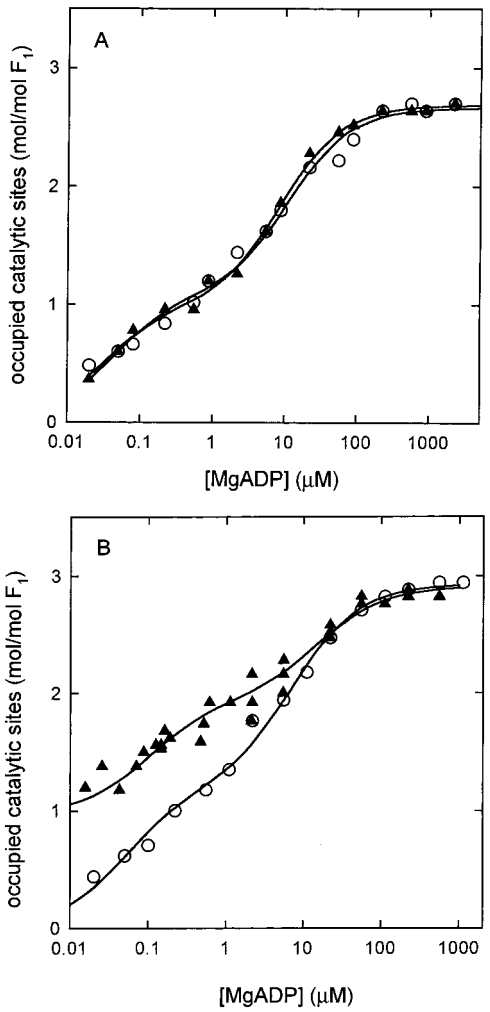

FIGURE 3: Binding of MgADP−fluoroaluminate to mutant F_1. (A) αR376Q/βY331W F_1; (B) αR376K/βY331W F_1. (▲) MgADP plus fluoroaluminate; (○) MgADP alone. The lines are fits to a model assuming two classes of sites (○, ▲ in panel A) as found previously for MgADP alone (*5, 29*), or (▲ in panel B) to a model assuming three sites, as found previously for MgADP−fluoroaluminate binding (*16*).

DISCUSSION

Arginine residues are crucial for many enzyme phosphoryl transfer reactions, and the aim of this study was to investigate one such arginine in F_1-ATPase, namely, α-Arg-376. Crystal structures of F_1 show that α-Arg-376 lies close to the phosphate groups of catalytic site-bound nucleotide (*3, 9*). In the "βTP" site (*3*), the NH1 nitrogen atom of the guanidinium group of α-Arg-376 is 3.1 Å from the nearest oxygen of the γ-phosphate and 3.4 Å from the β−γ bridging oxygen of bound nucleotide. In the "βDP" site, this nitrogen is 3.0 Å from the nearest oxygen of the β-phosphate, 3.2 Å from the nearest oxygen of the α-phosphate, and 3.3 Å from the α−β bridging oxygen. This location of α-Arg-376 within the catalytic site therefore suggests that it plays an essential role in catalysis. Hence, we constructed three mutants, αR376C/βY331W, αR376Q/βY331W, and αR376K/βY331W, to determine the role(s) of α-Arg-376 in greater detail. The βY331W mutation enabled us to measure catalytic site nucleotide-binding parameters of F_1 purified from these mutants because the genetically engineered β-Trp-331 residue acts as an intrinsic probe whose fluorescence signal is quenched upon binding of nucleotide at the catalytic sites.

The three mutations αR376C, αR376Q, and αR376K caused loss of ATP synthase activity in vivo and severely diminished rates of steady-state MgATP hydrolysis in vitro, demonstrating convincingly that α-Arg-376 is crucial for the catalytic mechanism of ATP synthase. The data confirmed previous reports of very low ATPase activity displayed by αR376C F_1 (*14, 15*) and show that neither Gln nor Lys can satisfactorily substitute for Arg at residue α-376.

Our measurements of catalytic site nucleotide binding parameters in the mutant enzymes indicated that α-Arg-376 normally plays no major functional role in providing binding energy for either MgATP or MgADP. None of the three mutations had any effect on MgATP binding at the highest affinity catalytic site, where the actual reaction is thought to occur. To cite two contrasting examples, we have previously shown that both β-Arg-182 and β-Lys-155, two positively charged residues which also lie close to the phosphate groups of catalytic site-bound nucleotide, provide substantial binding energy for MgATP via interaction with the γ-phosphate at the highest affinity site (*17, 29*). Substitution of either of

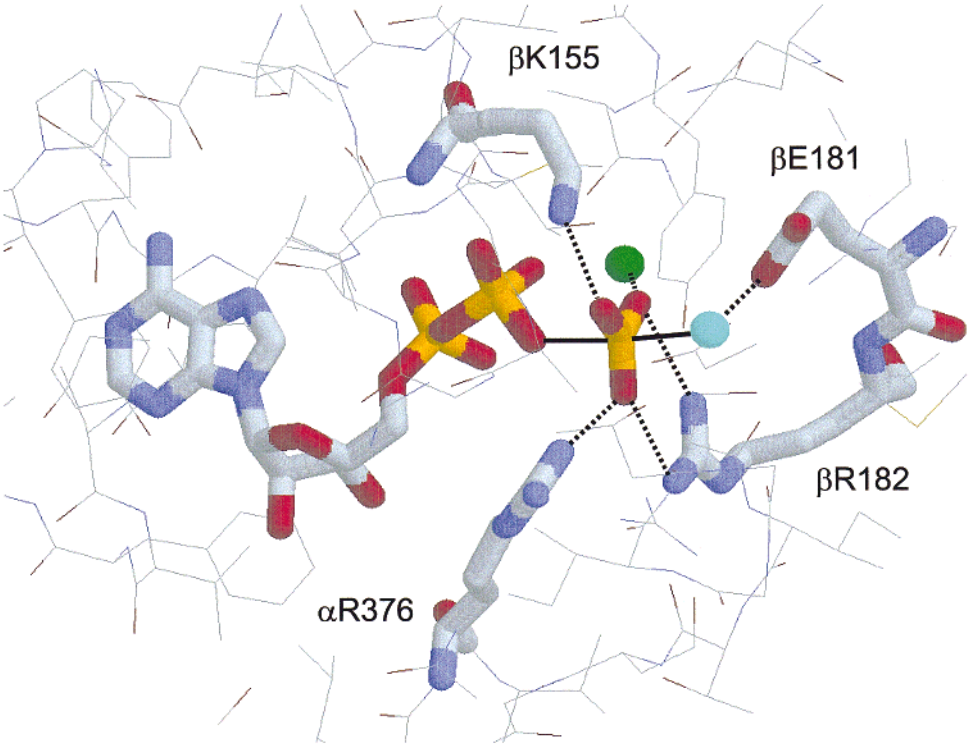

FIGURE 4: Model for the catalytic transition state of MgATP hydrolysis in F_1. A trigonal bipyramidal pentacoordinate phosphorus transition state is proposed. Mg^{2+} ion is green; the proposed attacking water is cyan. Residues β-Lys-155, β-Arg-182, and α-Arg-376 hydrogen-bond to the equatorial oxygens of the terminal phosphate. The axial (apical) bonds are shown in black. The water molecule is hydrogen-bonded to the carboxyl of β-Glu-181, which is proposed to immobilize, orient, and polarize it. Based on the "βTP" site in (*3*) and presented using RasMol software, kindly provided by Dr. Roger Sayle, Glaxo Research.

these by Gln caused large decreases in the binding affinity for MgATP at this site. Clearly, α-Arg-376 differs from β-Arg-182 and β-Lys-155 in this important respect. Given the proximity of α-Arg-376 in the X-ray structures to bound nucleoside di- and triphosphates, as detailed above, the results were surprising. The results with the Cys mutant do support the view that residue α-376 is close enough to the nucleotide for the negatively charged Cys and the nucleotide phosphates to engender mutual repulsion. It must be concluded, therefore, that the stereochemical constraints of the guanidinium group are sufficiently stringent that interaction does not occur with the nucleotide phosphates in the ground states, despite the apparent proximity.

The inability of the Gln and Cys mutants to bind the transition state analogue MgADP−fluoroaluminate provides firm evidence that a major role of the guanidinium group of α-Arg-376 is to stabilize the catalytic transition state, and failure to do so in these mutants accounts for loss of catalysis. In the Lys mutant, binding of MgADP−fluoroaluminate did occur, showing that the positively charged substituted side chain could still support formation of the transition state, and yet the Lys mutant enzyme was inactive. One likely explanation is that an additional function of residue α-Arg-376 is to transmit conformational signals across the α/β subunit catalytic interface as the hydrolysis reaction proceeds. It may be recalled that earlier workers had concluded this to be the main function of this residue (*14*, *15*), and that there is a body of literature attesting to the importance of such conformational signal transmission for steady-state catalysis (*2*, *17*). Through its direct interaction with the catalytic transition state, residue α-Arg-376 could act as a lever to induce relative α/β subunit movement as the ATPase reaction progresses from MgATP binding to the transition state and then to separation of products MgADP and P_i. It may be noted that α-Arg-376 is close to several other residues in the catalytic site. For instance, the NH1 nitrogen lies 3.1 and 2.8 Å from the carbonyl oxygen of residue α-Ile-346 in the βTP and βDP catalytic sites, respectively, and the proximity (3.0−3.4 Å) of one or the other of the α-Arg-376 NH nitrogens to atoms of residues α-Thr-349, α-Asp-350, and β-Arg-182 is also evident. Thus, the Lys mutant may support formation of the transition state, but be unable to carry out subsequent conformational movements properly because it lacks specific interactions with other residues endowed by the guanidinium group.

Taken in combination with recent work from our laboratory, the work presented here allows us to formulate a model for the structure of the catalytic transition state in ATP synthase, which is shown in Figure 4, and involves residue α-Arg-376 together with β-Lys-155, β-Arg-182, and β-Glu-181. Evidence for the involvement of the latter three residues in transition state stabilization was reported in refs *16* and *17*. We suggest that formation of the transition state involves the following considerations. As noted above, in contrast to α-Arg-376, both of the residues β-Lys-155 and β-Arg-182 provide binding energy for the substrate MgATP, largely through interaction with the γ-phosphate. We propose that during MgATP hydrolysis, β-Lys-155 and β-Arg-182 first interact with and orient the γ-phosphate of bound MgATP in the highest affinity site (as shown in Figure 1 of ref *17*). Residues β-Thr-156, β-Glu-185, and β-Asp-242, although not shown in Figure 4, are also important in the binding and orientation of the MgATP through their liganding of the Mg^{2+} ion (*30*). Concomitantly, the attacking water molecule

is immobilized, oriented, and polarized for nucleophilic attack upon the terminal phosphate by the carboxyl side chain of residue β-Glu-181, well-known to be essential for catalysis. Both residue β-Glu-181 and the putative attacking water were located in appropriate positions relative to the γ-phosphate in the X-ray structure by Abrahams et al. (*3*), and from subsequent work, it has been established that residue β-Glu-181 is not functionally involved in binding either MgATP or MgADP (*29, 30*), but is required for formation of the transition state (*16*). α-Arg-376, although lying close to the phosphate moiety of MgATP, does not participate in catalysis until formation of the transition state is initiated; then the side chain of α-Arg-376 moves toward the terminal phosphate of the pentacoordinate transition state species, and together with β-Lys-155 and β-Arg-182, hydrogen-bonds with one of the anionic equatorial oxygens and neutralizes the negative charge, yielding the structure of Figure 4.

It is interesting that the manner in which the α subunit in F_1-ATPase provides an arginine residue that inserts into the catalytic site formed largely by the adjacent β subunit mirrors the situation occurring in the G-proteins Ras and Rho (*11*−*13*). These G-proteins bind GTP in their catalytic sites, but have very low intrinsic GTPase activity, which is accelerated 10^5-fold by GTPase activating proteins (GAPs). GAPs bind to their cognate G-protein and insert an "arginine finger" residue into the catalytic site, which causes rate acceleration by stabilization of the catalytic transition state. The crystal structure of GAP complexed to the G-protein Cdc42Hs, containing the ground-state analogue GMPPNP in its catalytic site, shows that the arginine provided by the GAP has no interaction with the GMPPNP (*12*). However, when the transition state analogue GDP−fluoroaluminate is present in the catalytic site, a rearrangement of the Cdc42Hs/GAP interface occurs such that the essential arginine provided by the GAP is able to interact with the transition state analogue (*13*). The evidence presented here shows that a parallel situation occurs with α-Arg-376 in ATP synthase.

The requirement for α-Arg-376 to stabilize the catalytic transition state in F_1 provides an explanation as to why isolated β subunit has little or no intrinsic ATPase activity. Although isolated β subunit preparations from various sources show the ability to bind MgATP, they exhibit ATPase activities which are around 3 orders of magnitude lower than that of wild-type F_1 (*31, 32*). $\alpha\beta$ heterodimers exhibit higher activity than isolated β subunit preparations (*33, 34*). It is likely that this increased activity is due to the participation of α-Arg-376 in the catalytic site. Physiological rates are only achieved in $\alpha_3\beta_3\gamma$ complexes (*31, 34, 35*), implying that the presence of the γ subunit influences movement of α-Arg-376 into the catalytic site, perhaps as a result of rotation. It is also apparent that during assembly of F_1 from its component subunits in cells, potentially harmful ATP hydrolysis by isolated β subunit is prevented until α, β, and γ subunits are properly assembled together, a useful protective mechanism.

ACKNOWLEDGMENT

We thank Rachel Shaner, Christine Schaner, and Raajit Rampal for excellent technical assistance, and Dr. R. K. Nakamoto for plasmid pBWU13.4.

REFERENCES

1. Nakamoto, R. K. (1996) *J. Membr. Biol. 151*, 101−111.
2. Weber, J., and Senior, A. E. (1997) *Biochim. Biophys. Acta 1319*, 19−58.
3. Abrahams, J. P., Leslie, A. G. W., Lutter, R., and Walker, J. E. (1994) *Nature 370*, 621−628.
4. Penefsky, H. S., and Cross, R. L. (1991) *Adv. Enzymol. 64*, 173−214.
5. Weber, J., Wilke-Mounts, S., Lee, R. S. F., Grell, E., and Senior, A. E. (1993) *J. Biol. Chem. 268*, 20126−20133.
6. Löbau, S., Weber, J., and Senior, A. E. (1998) *Biochemistry 37*, 10846−10853.
7. Noji, H., Yasuda, R., Yoshida, M., and Kinosita, K., Jr. (1997) *Nature 386*, 299−302.
8. Boyer, P. D. (1989) *FASEB J. 3*, 2164−2178.
9. Bianchet, M. A., Hullihen, J., Pedersen, P. L., and Amzel, L. M. (1998) *Proc. Natl. Acad. Sci. U.S.A. 95*, 11065−11070.
10. Shirakihara, Y., Leslie, A. G. W., Abrahams, J. P., Walker, J. E., Ueda, T., Sekimoto, Y., Kamabara, M., Saika, K., Kagawa, Y., and Yoshida, M. (1997) *Structure 5*, 825−836.
11. Scheffzek, K., Ahmadian, M. R., Kabsch, W., Wiesmüller, L., Lautwein, A., Schmitz, F., and Wittinghofer, A. (1997) *Science 277*, 333−338.
12. Rittinger, K., Walker, P. A., Eccleston, J. F., Nurmahomed, K., Owen, D., Laue, E., Gamblin, S. J., and Smerdon, S. J. (1997) *Nature 388*, 693−697.
13. Rittinger, K., Walker, P. A., Eccleston, J. F., Smerdon, S. J., and Gamblin, S. J. (1997) *Nature 389*, 758−762.
14. Soga, S., Noumi, T., Takeyama, M., Maeda, M., and Futai, M. (1989) *Arch. Biochem. Biophys. 268*, 643−648.
15. Turina, P., Aggeler, R., Lee, R. S.-F., Senior, A. E., and Capaldi, R. A. (1993) *J. Biol. Chem. 268*, 6978−6984.
16. Nadanaciva, S., Weber, J., and Senior, A. E. (1999) *J. Biol. Chem. 274*, 7052−7058.
17. Nadanaciva, S., Weber, J., and Senior, A. E. (1999) *Biochemistry 38*, 7670−7677.
18. Downie, J. A., Cox, G. B., Langman, L., Ash, G., Becker, M., and Gibson, F. (1981) *J. Bacteriol. 145*, 201−208.
19. Vandeyar, M., Weiner, M., Hutton, C., and Batt, C. (1988) *Gene 65*, 129−133.
20. Ketchum, C. J., Al-Shawi, M. K., and Nakamoto, R. K. (1998) *Biochem. J. 330*, 707−712.
21. Senior, A. E., Latchney, L. R., Ferguson, A. M., and Wise, J. G. (1984) *Arch. Biochem. Biophys. 228*, 49−53.
22. Rao, R., Al-Shawi, M. K., and Senior, A. E. (1988) *J. Biol. Chem. 263*, 5569−5573.
23. Weber, J., Lee, R. S. F., Grell, E., Wise, J. G., and Senior, A. E. (1992) *J. Biol. Chem. 267*, 1712−1718.
24. Laemmli, U. K. (1970) *Nature 227*, 680−685.
25. Bradford, M. M. (1976) *Anal. Biochem. 72*, 248−254.
26. van Veldhoven, P. P., and Mannaerts, G. P. (1987) *Anal. Biochem. 161*, 45−48.
27. Weber, J., Wilke-Mounts, S., and Senior, A. E. (1994) *J. Biol. Chem. 269*, 20462−20467.
28. Senior, A. E., Lee, R. S. F., Al-Shawi, M. K., and Weber, J. (1992) *Arch. Biochem. Biophys. 297*, 340−344.
29. Löbau, S., Weber, J., Wilke-Mounts, S., and Senior, A. E. (1997) *J. Biol. Chem. 272*, 3648−3656.
30. Weber, J., Wilke-Mounts, S., Hammond, S. T., and Senior, A. E. (1998) *Biochemistry 37*, 12042−12050.
31. Al-Shawi, M. K., Parsonage, D., and Senior, A. E. (1991) *J. Biol. Chem. 265*, 5595−5601.
32. Harris, D. A., Boork, J., and Baltscheffsky, M. (1985) *Biochemistry 24*, 3876−3883.
33. Andralojc, P. J., and Harris, D. A. (1993) *Biochim. Biophys. Acta 1143*, 51−61.
34. Miwa, K., and Yoshida, M. (1989) *Proc. Natl. Acad. Sci. U.S.A. 86*, 6484−6487.
35. Dunn, S. D., and Futai, M. (1980) *J. Biol. Chem. 255*, 113−118.

BI9917683